nature sustainability

Article

https://doi.org/10.1038/s41893-023-01206-5

Carbon emissions of 5G mobile networks in China

Received: 26 February 2023

Accepted: 21 July 2023

Published online: 17 August 2023

Check for updates

Tong Li[1], Li Yu[2], Yibo Ma[1], Tong Duan[3], Wenzhen Huang[1], Yan Zhou[2], Depeng Jin[1], Yong Li[1] ✉ & Tao Jiang[4] ✉

Telecommunication using 5G plays a vital role in our daily lives and the global economy. However, the energy consumption and carbon emissions of 5G mobile networks are concerning. Here we develop a large-scale data-driven framework to quantitatively assess the carbon emissions of 5G mobile networks in China, where over 60% of the global 5G base stations are implemented. We reveal a carbon efficiency trap of 5G mobile networks leading to additional carbon emissions of 23.82 ± 1.07 Mt in China, caused by the spatiotemporal misalignment between cellular traffic and energy consumption in mobile networks. To address this problem, we propose an energy-saving method, called DeepEnergy, leveraging collaborative deep reinforcement learning and graph neural networks, to make it possible to effectively coordinate the working state of 5G cells, which could help over 71% of Chinese provinces avoid carbon efficiency traps. The application of DeepEnergy can potentially reduce carbon emissions by 20.90 ± 0.98 Mt at the national level in 2023. Furthermore, the mobile network in China could accomplish more than 50% of its net-zero goal by integrating DeepEnergy with solar energy systems. Our study deepens the insights into carbon emission mitigation in 5G networks, paving the way towards sustainable and energy-efficient telecommunication infrastructures.

Connectivity has become a defining feature of modern economies and societies[1]. Mobile networks using 5G play a big role by providing high network capacity and ubiquitous digital connectivity for a massive number of terminals[2], such as smartphones, vehicles and sensors. Connectivity through 5G will usher in a new era of the digital economy, unlocking a series of innovative services, including health care[3], autonomous vehicles[4], smart cities[5] and intelligent manufacturing[6].

However, the impact of 5G mobile networks on energy consumption and carbon emissions is a matter of concern. Compared with previous generations of mobile networks, 5G networks have more antennas[7] and larger bandwidths[8], dramatically increasing the energy consumption of base stations. China Mobile's measurement report[9] indicates that the energy consumption of a 5G base station is 4.3 kWh, which is four times that of a 4G base station at 1.1 kWh. One 5G base station is estimated to produce 30 t of carbon emissions in one year of operation[10]. Thus, 5G networks in China are roughly estimated to produce over 60 Mt of carbon emissions annually at the national level[11]. Such high energy consumption and carbon emissions may cause severe environmental problems and conflict with global sustainable development goals (SDGs)[12]. Nevertheless, only a handful of studies have made initial attempts to analyse the carbon emissions of 5G[10,13]. These studies have discussed the carbon emissions of a single 5G base station from the whole life cycle perspective, but they have been limited due to the lack of comprehensive and systematic investigations supported by detailed real-world data. To reveal and quantify the greenhouse impacts caused by 5G networks and explore a sustainable development pathway for

[1]Beijing National Research Center for Information Science and Technology (BNRist), Department of Electronic Engineering, Tsinghua University, Beijing, China. [2]China Mobile Research Institute, Beijing, China. [3]National Digital Switching System Engineering and Technological Research Center, Zhengzhou, China. [4]Research Center of 6G Mobile Communications, Huazhong University of Science and Technology, Wuhan, China. ✉e-mail: liyong07@tsinghua.edu.cn; taojiang@hust.edu.cn

mobile networks in China, more detailed and concrete evidence from large-scale real-world data is needed[14].

In this Article, we delve into the sustainability of 5G mobile networks in China, aiming to find an environmentally friendly method to launch and operate 5G mobile networks. To quantify carbon emissions induced by mobile networks, we propose a data-driven, simulation-based model that considers the interactions between mobile communication and power generation systems. Using large-scale real-world network data from Nanchang, a provincial capital in China, we discover the energy efficiency trap caused by the launch of 5G (Supplementary Fig. 1). Energy efficiency[2,9,15] is defined as the ratio of mobile network traffic to energy consumption. Our simulation-based model indicates that China is expected to consume an extra 35.02 ± 0.33 TWh of energy, equivalent to an additional 23.82 ± 1.07 Mt of carbon emissions, due to the efficiency trap. We next identify that the decrease in energy efficiency is primarily due to the exacerbated misalignment between cellular traffic and energy consumption. To mitigate the misalignment and improve energy efficiency, we propose DeepEnergy, an energy-saving method leveraging collaborative deep reinforcement learning and graph neural networks, to adaptively control the working state of base stations on the basis of their dynamic traffic loads. Our study paves the way to achieving SDGs and future net-zero mobile networks by providing insight into carbon emission mitigation in 5G network infrastructure operations.

Results

Launching 5G leads to a carbon efficiency trap

We quantified and estimated the carbon emissions of mobile network operations in Nanchang from 2020 to 2023 (Methods). As illustrated in Fig. 1a, the launch of 5G resulted in an increase in daily network capacities from 12 PB (12,264 4G base stations) to 22 PB (12,264 4G base stations and 2,159 5G base stations). The operation of the newly launched 5G base stations has led to a sharp increase in energy consumption and a decline in energy efficiency (Supplementary Fig. 1). Correspondingly, there has been a dramatic increase in daily carbon emissions of 178 t after launching 5G (Fig. 1b). Carbon efficiency, the amount of network traffic that can be delivered for one unit of carbon emissions, decreased from 2.98 TB per tCO_2 to 2.08 TB per tCO_2 (Fig. 1c). After the launch of the 5G network, there was a large and rapid increase in carbon emissions. However, the traffic load did not grow to the same extent, exacerbating the misalignment between cellular network traffic and energy consumption; this is the critical reason for the lowered carbon efficiency of the mobile network. Although the carbon efficiency did increase over time as mobile users consumed more network traffic, we estimated that Nanchang took more than six months to return to its pre-5G level of carbon efficiency. This decrease in carbon efficiency and subsequent recovery process is referred to as the carbon efficiency trap, as depicted by the grey shaded area in Fig. 1c. In the carbon efficiency trap, the mobile network produces additional carbon emissions to carry the same network traffic due to reduced carbon efficiency. In Nanchang, for example, the efficiency trap was estimated to cause an additional 13.11 ± 0.74 kt of carbon dioxide emissions.

The energy consumption of a mobile network depends on the number of base stations (Supplementary Fig. 2). We next generalized the simulation results from Nanchang to all provinces in China using the Monte Carlo method by considering the number of 4G and 5G base stations in each province (Methods). The uncertainty in carbon emissions caused by mobile networks in each province is approximately −6% and +6% at the 95% confidence level (see Supplementary Tables 7 and 16 for the details). According to the estimation results, the eastern provincial regions have a higher number of 5G base stations and generate more additional carbon emissions (Fig. 1d,e). Guangdong, Jiangsu and Zhejiang are the top three contributors, each accounting for 0.13, 0.11 and 0.08 of the national carbon emissions. In contrast, the western provincial regions (such as Qinghai and Tibet) have fewer 5G base stations and produce fewer additional carbon emissions. The wealthier eastern provincial regions also have higher additional carbon emissions per unit area than the less developed western areas (Fig. 1f). Tibet has the lowest additional carbon emissions per unit area of 0.0155 $tCO_2\ km^{-2}$, whereas Shanghai's additional carbon emissions per unit area are roughly 10,811 times higher (167.58 $tCO_2\ km^{-2}$). Notably, each square kilometre of forest can only absorb approximately 500 tCO_2 per year[16]. In other words, the additional carbon emissions caused by the launch of 5G in Shanghai would require a forest the same size as Shanghai city to take at least four months to absorb. Therefore, on the basis of the intensity and density of additional carbon emissions, China (especially the eastern provincial regions) may face severe environmental issues that may cause irreversible damage during the launch of 5G. We urgently need to dig into the root causes and find a solution to launch and operate 5G networks sustainably.

Traffic and energy show huge spatiotemporal misalignment

To uncover the causes of the carbon efficiency trap, we investigated the spatiotemporal misalignment between cellular traffic and energy consumption, which occurs when the energy consumption of a mobile network is not directly proportional to the traffic load. Taking the network traffic data of Nanchang as an example, Fig. 2a shows how the energy consumed by the mobile network varies with the aggregated traffic load. Even with light traffic of 2.5 TB (that is, 1% of the network capacity), the energy consumption is relatively high at 25.6 MWh, roughly 42% of the maximum energy consumption. A mobile network reaches its maximum energy consumption, denoted by E_{max}, when the carried traffic reaches its available capacity C. In contrast, the desired energy consumption[17], which is proportional to the traffic load (the green dashed line in Fig. 2a), is much less, at only about 0.6 MWh for light traffic of 2.5 TB. To measure the misalignment between traffic load L and energy consumption E, we defined a metric called the misalignment factor, denoted by $M = \tilde{E} - \tilde{L}$, where $\tilde{E} = E/E_{max}$ represents the normalized energy consumption and $\tilde{L} = L/C$ represents the normalized traffic load. The misalignment factor is in the interval [0, 1] to measure the discrepancy between normalized energy consumption and traffic load (see Supplementary Note 1 for the details). This discrepancy is more severe as the factor increases. When $M = 0$, the energy consumption is directly proportional to the traffic load, and there is no misalignment.

The misalignment factor between traffic load and energy consumption changes over time and space. As illustrated in Fig. 2b, the misalignment factor shows an apparent daily pattern, with higher values at night and lower values during the day. Specifically, the misalignment factor of 5G networks (0.68) is much higher than that of 4G networks (0.49), increasing the misalignment factor of the entire mobile network to 0.56 on average. Regarding spatial distribution, the misalignment factors of 5G networks are higher in the city centre, where the 5G base stations are more concentrated (Fig. 2d). The misalignment factors of 4G networks are generally uniformly distributed, with low values (Fig. 2c). Thanks to years of optimization of 4G base station deployments, the energy consumption of 4G base stations has a similar spatial distribution to the traffic loads (Supplementary Fig. 3). In contrast, due to the insufficient traffic profiles of 5G applications, the deployment of 5G base stations is not yet optimized, which leads to extremely high misalignment factors (often exceeding 0.8) in most regions.

Given a mobile network's traffic load L, the energy efficiency, denoted by $\eta^{energy}(L)$, can be expressed as $\eta^{energy}(L) = \eta^{energy}_{desired}/(1 + M/\tilde{L})$, where $\eta^{energy}_{desired} = C/E_{max}$ denotes the desired energy efficiency of that mobile network (see Supplementary Note 1 for the details). The energy efficiency is thus affected by three key factors: $\tilde{L}$, $\eta^{energy}_{desired}$ and M. Specifically, $\eta^{energy}_{desired}$ depends on the technologies used in the mobile network. Thanks to the advanced technologies of 5G, such as massive multiple-input/multiple-output and subframe silence[18], the desired energy efficiency of 5G is 6.29 TB MWh^{-1}, which is twice that of 4G

https://doi.org/10.1038/s41893-023-01206-5

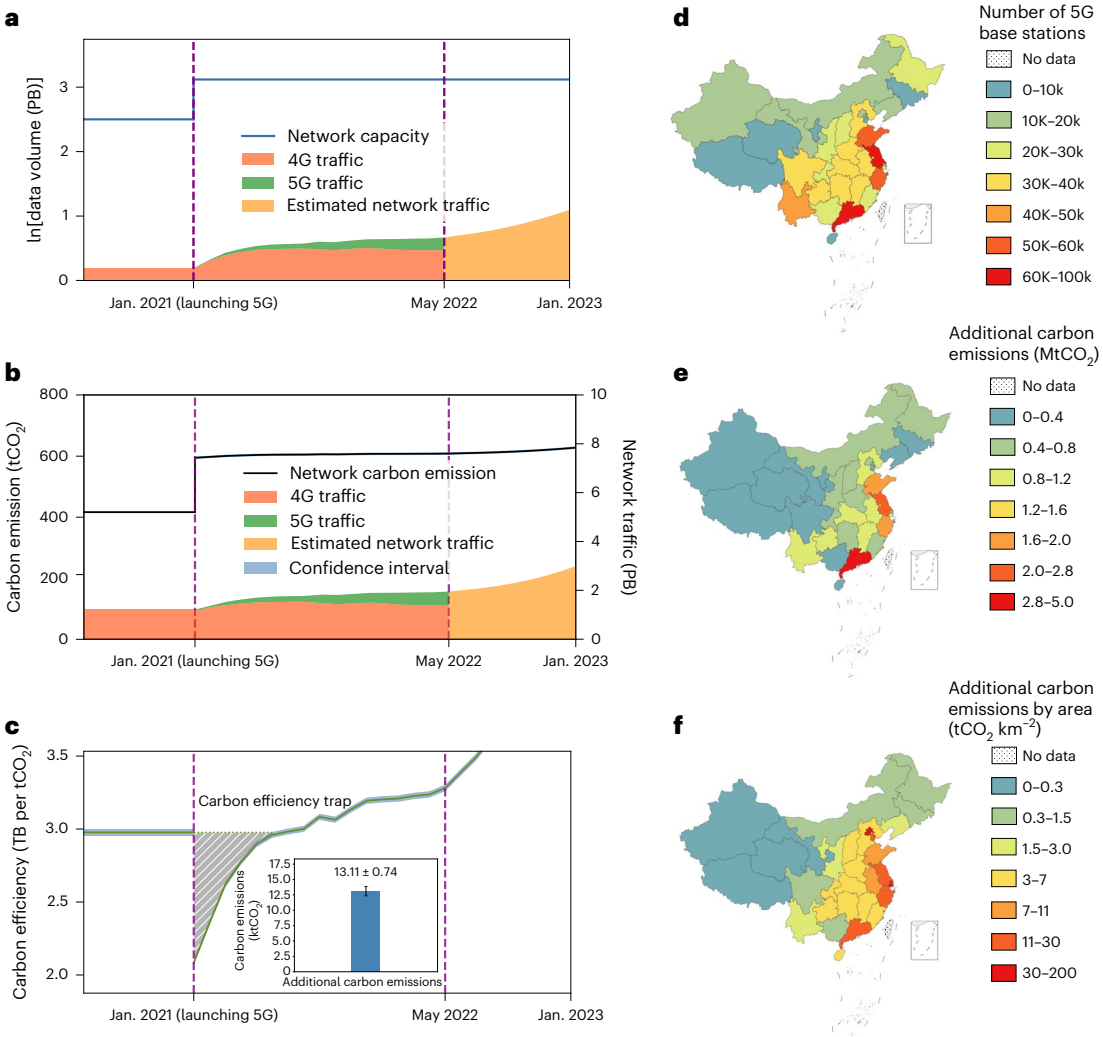

Fig. 1 | Analysis of carbon efficiency after the launch of 5G networks. **a**, Launching 5G led to a substantial increase in daily network capacities in Nanchang. **b**, The operation of the newly launched 5G base stations led to a sharp increase in carbon emissions in Nanchang. **c**, Launching 5G led to the appearance of a carbon efficiency trap and caused additional carbon emissions of 13.11 ± 0.74 $ktCO_2$ in Nanchang. **d**, The number of 5G base stations across different provinces in China. **e**, The amount of additional carbon emissions across different provinces in China. **f**, The amount of additional carbon emissions per unit area across different provinces in China.

(3.01 TB MWh^{-1}). However, the rise in the misalignment factor reduces the energy efficiency. As illustrated in Fig. 2f–h, regions with large misalignment factors exhibit low energy efficiency and vice versa. The average energy efficiency of the city centre falls from 2.98 TB MWh^{-1} (4G networks) to 1.94 TB MWh^{-1} (covering both 4G and 5G networks), corresponding to the increase in the misalignment factor. In summary, launching 5G networks increases the misalignment between traffic load and energy consumption and lowers the energy efficiency of the entire mobile network. Figure 2i,j depicts one-week patterns of 4G and 5G networks for traffic loads, energy consumption in the real world and the desired energy consumption without misalignment. The traffic loads of both 4G and 5G exhibit a diurnal rhythm, whereas the network energy consumption remains almost constant throughout the day. Such findings are consistent with Fig. 2a. There is also a vast gap between the current energy consumption with huge misalignment and the desired energy consumption without misalignment (the shaded areas in Fig. 2i,j), indicating a remarkable potential to reduce energy consumption and increase energy efficiency by addressing the spatiotemporal misalignment between cellular traffic and energy consumption in mobile networks.

Energy-saving methods mitigate misalignment and the carbon efficiency trap

The main factor behind the misalignment between traffic and energy is that the energy consumption of the cooling devices and fixed radio transmission overhead at the base stations is unaffected by traffic load (see Supplementary Note 2 for the details). One solution to mitigate the misalignment is to switch the base stations into low-power operation mode by proactively turning off some components, such as the power amplifier and cooling devices, when the traffic load is relatively low. This low-power operation mode is known as sleep mode[19]. Notably, a base station in sleep mode cannot provide service. Other active compensation base stations nearby must therefore handle mobile users who were previously served by the base station in sleep mode (see Supplementary Note 4 for the details).

We propose an artificial intelligence (AI) empowered energy-saving method, DeepEnergy, which is based on collaborative deep reinforcement learning to control the working state of cells adaptively (Methods). A cell is a carrier on a sector of a base station. A base station generally has multiple cells. Specifically, DeepEnergy models each cell as an intelligent agent that self-decides its working state on the

https://doi.org/10.1038/s41893-023-01206-5

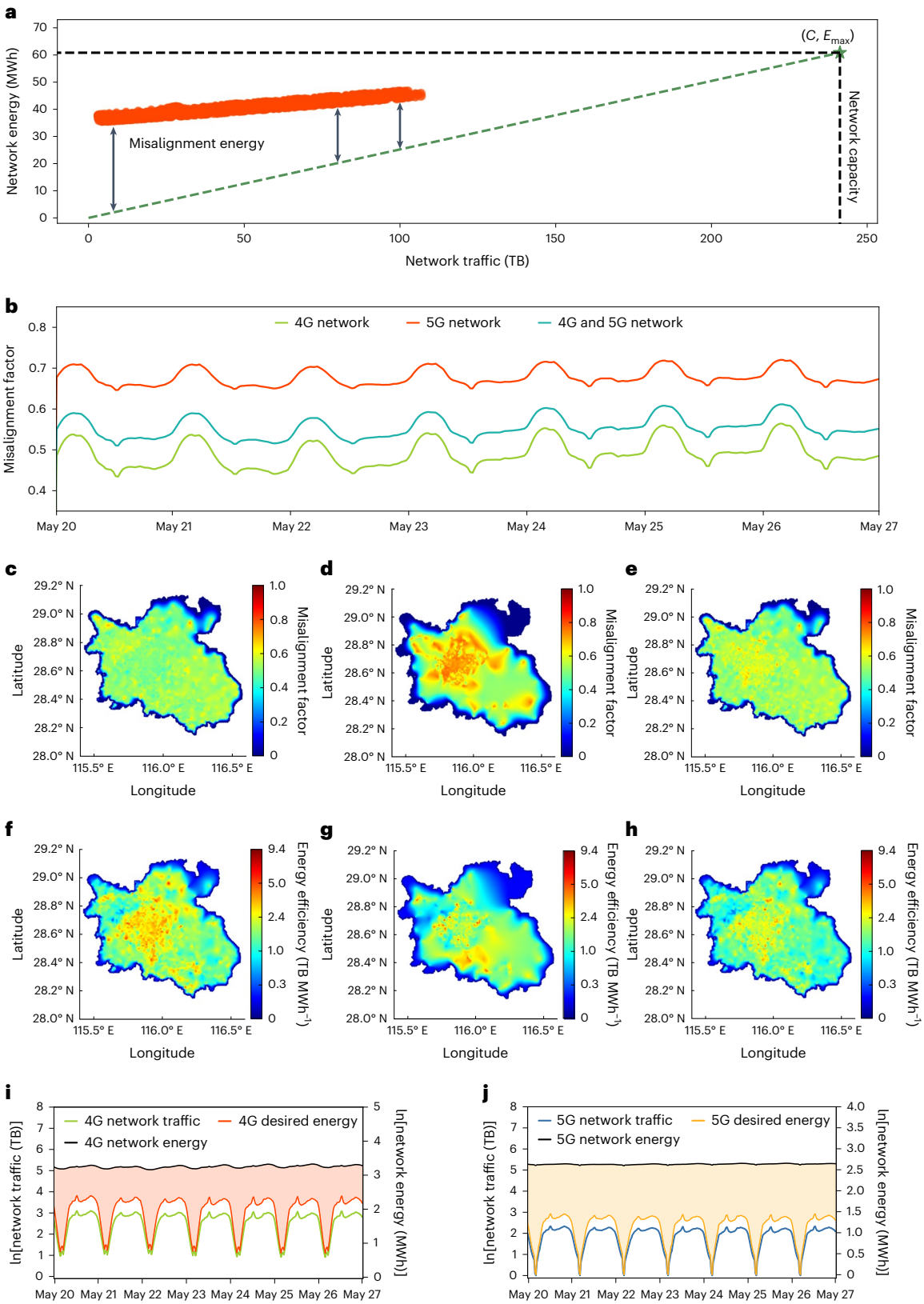

Fig. 2 | Cellular traffic and energy consumption show huge spatiotemporal misalignment. a, The energy–traffic curve for mobile networks is based on the network performance data collected in Nanchang. Network energy is not proportional to its carried traffic load, showing the misalignment between traffic and energy. **b**, One-week misalignment factor pattern of mobile networks. The launch of 5G networks causes the mobile network's misalignment factor to rise. **c**, Spatial distribution of misalignment factors of 4G networks. **d**, Spatial distribution of misalignment factors of 5G networks. **e**, Spatial distribution of misalignment factors of the entire mobile network. **f**, Spatial distribution of energy efficiency of 4G networks. **g**, Spatial distribution of energy efficiency of 5G networks. **h**, Spatial distribution of energy efficiency of the entire mobile network. Regions with large misalignment factors exhibit low energy efficiency and vice versa. **i**, One-week traffic and energy pattern of the 4G network. **j**, One-week traffic and energy pattern of the 5G network. Addressing the spatiotemporal misalignment between cellular traffic and energy consumption in mobile networks could significantly reduce energy consumption.

basis of traffic loads. DeepEnergy aims to learn an action-value network for cells, which would help quantify how much energy could be saved from each cell's working state decision. Since the mobile network is enormous and cells may interact with each other, DeepEnergy adopts a collaborative grid-based learning strategy to learn the action-value network. DeepEnergy divides the region into small grids on the basis of the compensation relationships of cells. The cells in each grid are equivalent in service capability and thus can act as collaborative compensation cells for each other. Moreover, DeepEnergy models the attribution relationships between cells and base stations. As a result, DeepEnergy considers both intra-grid and intra-base-station collaboration among cells, making it possible to effectively coordinate the working state of tens of thousands of cells.

We compared DeepEnergy with two classical energy-saving methods: the threshold-based method[20] and the greedy method[17] (see Supplementary Note 4 for the details). Overall, DeepEnergy outperforms the other methods on the entire mobile network, consisting of 4G and 5G, reducing the misalignment factors from 0.56 to 0.28 on average (Fig. 3e). The threshold-based method performs the worst because there is no inter-cell collaboration, and cells independently decide whether to enter sleep mode on the basis of a predefined traffic load threshold. As a result, the threshold-based method can only barely work at night, when base station traffic is typically low (Fig. 3a). Alternatively, the greedy method considers intra-grid collaboration and has a comparable performance to that of DeepEnergy (Fig. 3c). Regarding the spatial distribution, DeepEnergy performs noticeably better in the city centre, with a misalignment factor of 0.22, which is much lower than those of the greedy method (0.53) and the threshold-based method (0.41) (Fig. 3b,d,f). This is because the city centre's base station density is comparatively high. DeepEnergy considers both intra-grid and intra-base-station collaborations of cells, making it more effective in dealing with regions with dense base station deployments and complex interactions between cells. Considering that the average density of 5G base stations is expected to be three times higher than that of 4G in the future[9], DeepEnergy has greater potential for energy savings in future mobile networks with very high base station densities.

Owing to the reduction in misalignment factors, DeepEnergy significantly improves the energy efficiency and carbon efficiency of mobile networks, reaching 2.83 TB MWh^{-1} and 4.16 TB per tCO_2, almost doubled in comparison to the case without energy saving (Fig. 3g). We next generalized the results from Nanchang to all provinces in China (Methods). Our results show that energy-saving methods can reduce the additional carbon emissions caused by launching 5G in China from 23.82 ± 1.07 Mt to 11.34 ± 0.46 Mt (threshold), to 4.24 ± 0.17 Mt (greedy) and to 0.18 ± 0.01 Mt (DeepEnergy). Specifically, DeepEnergy can help more than 71% of provinces in China successfully avoid the energy efficiency trap without producing additional carbon emissions (Fig. 3h). In addition, applying DeepEnergy would continue to reduce carbon emissions every year, with estimated reductions of 25.12 out of 50.52 Mt (2021), 24.65 out of 51.03 Mt (2022) and 20.90 out of 55.42 Mt (2023) at the national level (see Supplementary Tables 9–11 and 16 for the details).

Renewable energy helps achieve net-zero mobile networks

Due to diurnal rhythms, DeepEnergy performs better at night than in the daytime (Fig. 4a). Also, with the increase in traffic, the carbon reduction ratio decreases significantly during the day, dropping below 0.3 when the traffic load reaches 90% of network capacity. DeepEnergy thus has limitations in terms of energy saving during the daytime. Fortunately, the photovoltaic (PV) power system can operate during the day and provide renewable energy to the mobile network, further reducing carbon emissions in the daytime (Fig. 4b). When PV panels are deployed on base stations[21], DeepEnergy and the PV power system can work together to reduce carbon emissions both day and night.

We next assessed the carbon efficiency of the mobile network in Nanchang when we jointly operated DeepEnergy and the PV system through our proposed simulation-based system. Specifically, we located PV panels at each base station and used PVWatts[22,23] to estimate the potential electricity generation of the PV system (Methods). Figure 4c depicts the carbon efficiency of PV systems with various sizes of PV panels for DeepEnergy and the case without energy saving. The carbon efficiency of PV systems using DeepEnergy is much higher than in the case without energy saving. The overall carbon efficiency increases as cellular traffic increases. The gap in carbon efficiency between DeepEnergy and the case without energy saving widens from 1.50 TB per tCO_2 to 3.12 TB per tCO_2 when the traffic load reaches 90% of network capacity. Combining DeepEnergy and PV systems can therefore significantly improve the carbon efficiency of a mobile network.

The establishment of PV systems must take into account the economic investment[24]. We next estimated the costs of construction and maintenance of PV systems and showed how system performance changes with various economic investments. As illustrated in Fig. 4d, as investment increases, the mobile network becomes closer to the goal of net zero. The mobile network is estimated to achieve over 50% of its net-zero targets with DeepEnergy and a PV system when the annual investment contributed to the PV system is 13.85 million CNY. However, as the size of the PV system increases, the energy curtailment will become severe[25,26], lowering the cost efficiency due to marginal utility. We found that applying solar energy alone to reduce carbon emissions is not enough to achieve cost-effectiveness, with a levelized cost of carbon abatement of 308.18 CNY per tCO_2. The levelized cost of carbon abatement can be reduced to about one ninth, or 34.29 CNY per tCO_2, when we integrate DeepEnergy. As a result, DeepEnergy can help solar energy become an affordable path towards net-zero mobile networks in terms of cost efficiency.

Discussion

Our study reveals that the launch of 5G will lower the energy efficiency of the entire mobile network due to the high misalignment between traffic loads and energy consumption. The decline in energy efficiency will result in substantial additional energy consumption and carbon emissions, causing irreparable environmental harm. We therefore urgently need an environmentally friendly launch and operation strategy and must alter how we currently launch and operate 5G mobile networks. This paper proposes an energy-saving method, DeepEnergy, to proactively control base stations' working states on the basis of their dynamic traffic loads. DeepEnergy can mitigate the misalignment between traffic and energy in mobile networks, remarkably improving energy efficiency. As a result, in addition to assisting cities in avoiding energy efficiency traps, DeepEnergy continues to reduce energy consumption over time. For instance, it is estimated that from January 2021 to January 2023, the energy efficiency gain of Nanchang introduced by DeepEnergy would rise from 1.41 TB MWh^{-1} to 3.73 TB MWh^{-1}, and DeepEnergy would reduce energy consumption by 30.74 TWh in 2023. Furthermore, by integrating DeepEnergy and solar energy, the mobile network is estimated to accomplish over 50% of its net-zero target. DeepEnergy can thus assist in the launch of 5G and make the process of updating the mobile network infrastructure more environmentally friendly. The application of DeepEnergy could have reduced carbon emissions by 70.67 ± 3.64 Mt at the national level from 2021 to 2023 in China. However, there are several potential obstacles that might be encountered when implementing DeepEnergy. First, DeepEnergy is a machine learning model requiring significant data to train and optimize. The availability and quality of the data could be a potential limitation. Second, implementing DeepEnergy at scale would require computational resources and technical expertise, which could be hard to achieve for some organizations. Finally, operators may emphasize encouraging the usage of 5G networks and be reluctant to set 5G base stations to sleep, which may cause the operators to forgo DeepEnergy for commercial reasons.

https://doi.org/10.1038/s41893-023-01206-5

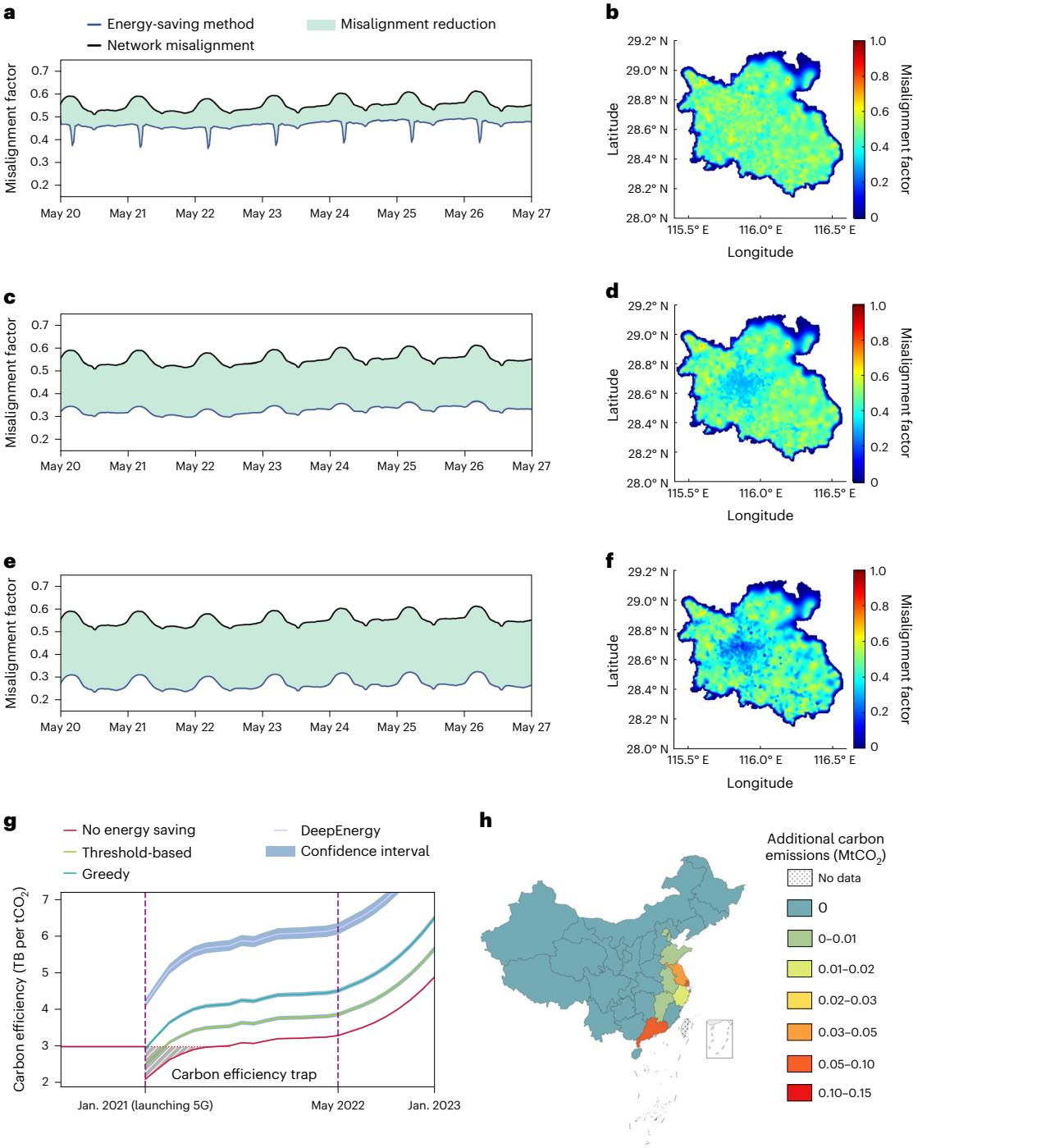

Fig. 3 | Performance analysis of energy-saving methods. a, Temporal distribution of misalignment factors of the entire mobile network in Nanchang using the threshold-based energy-saving method. **b**, Spatial distribution of misalignment factors of the entire mobile network in Nanchang using the threshold-based energy-saving method. **c**, Temporal distribution of misalignment factors of the entire mobile network in Nanchang using the greedy energy-saving method. **d**, Spatial distribution of misalignment factors of the entire mobile network in Nanchang using the greedy energy-saving method. **e**, Temporal distribution of misalignment factors of the entire mobile network in Nanchang using DeepEnergy. **f**, Spatial distribution of misalignment factors of the entire mobile network in Nanchang using DeepEnergy. **g**, The energy-saving methods have effectively improved carbon efficiency, and the DeepEnergy method can effectively avoid the carbon efficiency trap caused by launching the 5G network. **h**, The amount of additional carbon emissions across different provinces in China after using DeepEnergy. Twenty-two provinces have zero additional carbon emissions, and the others see notable reductions in additional carbon emissions.

SDGs are an urgent call to action for all industries. Our study quantifies the environmental impacts of launching 5G mobile networks and proposes a practical approach to achieve the SDGs in mobile networks by integrating energy-saving methods and solar energy systems. Our study offers a firm foundation for further research into the environmental deployment and operation of 5G networks. Additionally, as newer AI architectures and more powerful reinforcement learning models continue emerging, our study opens the door for developing

https://doi.org/10.1038/s41893-023-01206-5

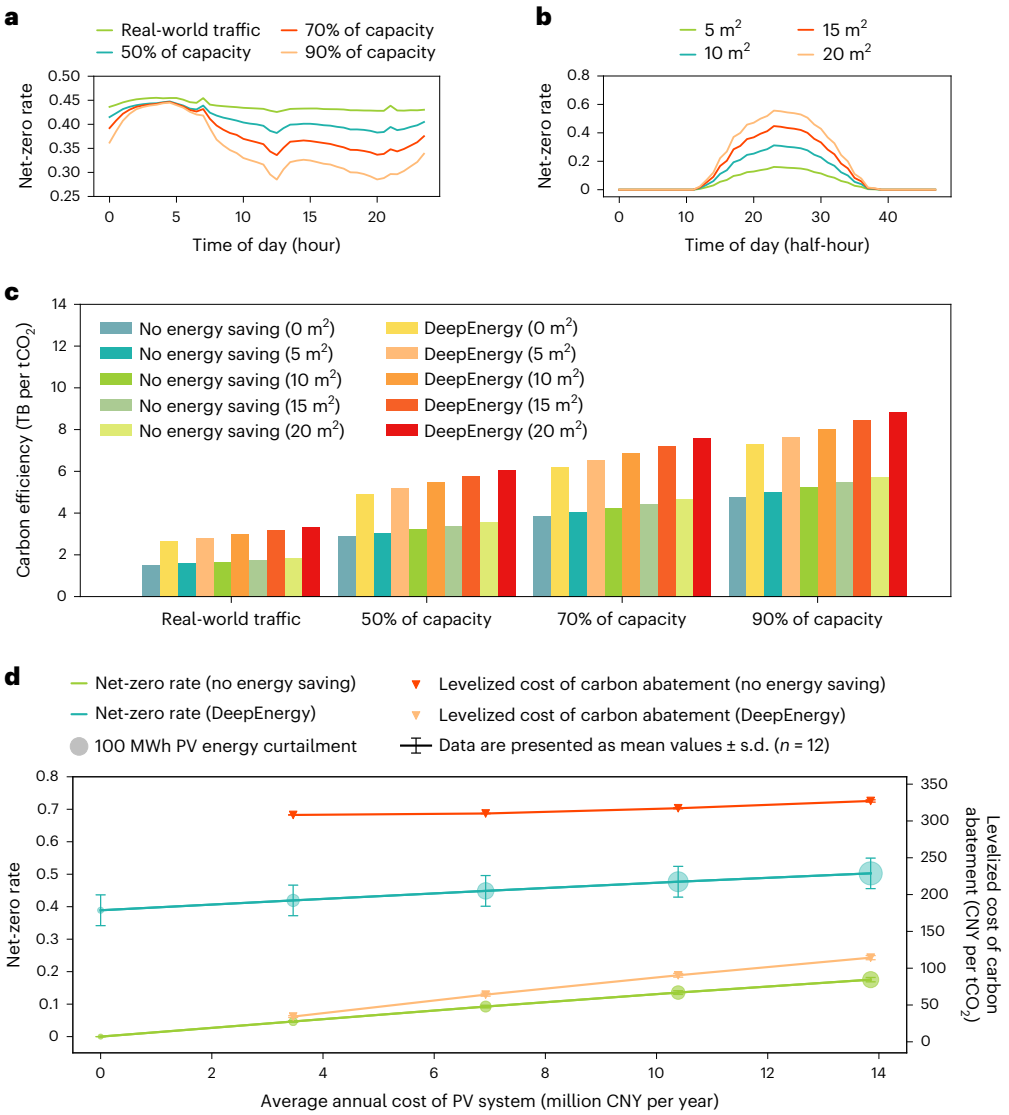

Fig. 4 | Renewable energy helps achieve net-zero mobile networks. a, Net-zero rate using DeepEnergy in a day under different traffic loads. The values 50%, 70% and 90% of capacity refer to future counterfactual cases of change in traffic volume. For example, 50% of capacity means that the maximum traffic volume of each cell in a day reaches 50% or above its capacity. The performance of DeepEnergy at night is superior to that in the daytime due to diurnal rhythms. **b**, Net-zero rate of a PV system in a day under different panel sizes. PV power generation systems can operate in the daytime and deliver clean energy to the mobile network. **c**, The carbon efficiency of the DeepEnergy scenario versus the no-energy-saving scenario for various PV systems. Combining DeepEnergy and the PV system can significantly improve the carbon efficiency of a mobile network. **d**, Net-zero rates and levelized cost of carbon abatement under different economic investments in the PV system. The radius of each circle represents the energy curtailment for the solar energy system.

more sophisticated systems for carbon emission reduction in mobile networks. The cost of deploying AI algorithms on base stations is much lower than the investment in renewable energy equipment, making it more affordable for developing countries to launch 5G in an environmentally friendly way. AI technologies therefore not only help achieve the SDGs in mobile networks due to their superior performance but also mitigate digital inequality among developed and developing countries because of low deployment costs.

As an initial attempt, our study still has some limitations. Our analysis was conducted on the basis of real-world datasets collected from China Mobile. The carbon emissions of mobile networks are underestimated because China Mobile accounts for only a portion of the market share (over 58%). We generalized the simulation results from Nanchang to all the provinces in China, which causes uncertainty. Renewable energy resources in different provinces are expected to be uneven. Many regions in western China have abundant indigenous renewable energy resources. The uncertainty resulting from differences in the distribution of energy resources will affect the path towards net-zero goals. In China, the deployment of new 5G base stations is still ongoing. Our study examined only the first wave of 5G base station launches, which may lead to an underestimation of carbon emissions.

Methods

Datasets

We simulated the carbon emissions from mobile networks in Nanchang and then extrapolated the results to all provinces in China. We collected the following data to conduct the investigation: energy consumption data of base stations, network traffic data in Nanchang, and the numbers of base stations and mobile users in each province (see Supplementary Note 0 for the details). Energy consumption data are essential for building the energy consumption model of base stations. We collected the data from 300 4G base stations and 266 5G base

stations in real-world mobile networks over one week in May 2022. The network traffic data were collected from China Mobile. We carried out a city-level measurement in Nanchang and collected fine-grained records on the network traffic of all 4G and 5G base stations for one week in May 2022. The network traffic data cover 12,264 4G base stations and 2,159 5G base stations. Monthly data on the numbers of base stations and mobile users in each province are released by the Ministry of Industry and Information Technology of the People's Republic of China[27].

Energy consumption model of base stations

Base stations are fundamental elements of mobile networks and are their principal energy consumers[9]. A base station generally consists of communication and supporting subsystems (see Supplementary Fig. 7 for the details). The remote radio unit (RRU) and baseband unit (BBU), major components of the communication subsystem, are responsible for transceiving radio signals and processing baseband signals, respectively. A base station may have several RRUs and BBUs. The cooling and other auxiliary devices are part of the supporting subsystem. The cooling equipment, such as air conditioning, keeps the base station at a proper operating temperature. The total power consumption P_{BS} of a base station can be calculated as follows:

$$P_{BS} = P_{tx} + P_{cooling}, \tag{1}$$

where P_{tx} denotes the power consumption of the communication subsystem and $P_{cooling}$ denotes the power consumed by cooling equipment to maintain an appropriate operating temperature. In this paper, we modelled only the cooling devices for the supporting subsystem because they account for over 90% of the supporting subsystem's power consumption[28].

P_{tx} is dominated by two components:

$$P_{tx} = P_{BBU} + P_{RRU}, \tag{2}$$

where P_{RRU} varies according to the amount of base station traffic. When the traffic load is heavy, RRUs have to consume more power to support more active physical resource blocks (PRBs). Baseband processing is handled by BBUs. P_{BBU} is proportional to the number of BBUs equipped at base stations. No matter how many PRBs are active, their power consumption remains constant and does not change in response to base station traffic (see Supplementary Note 2 for the details).

According to the energy consumption data of base stations, P_{RRU} varies from 200 W to 1,200 W and shows a linear relation with transmit power P_{trans} (Supplementary Figs. 9 and 11):

$$P_{RRU} = \alpha \times P_{trans} + \gamma, \tag{3}$$

where α and γ denote the slope and offset, respectively. In practice, α depends on the power amplifier efficiency of base stations, and γ depends on fixed circuit power[29]. Different base station types have specific coefficients in the linear regression model, as shown in Supplementary Tables 21 and 22.

P_{trans} ranges from 0 W to 300 W. We found that P_{trans} varies with the PRB usage ratio (r_{PRB}), and a linear regression model can approximate this relationship (Supplementary Figs. 12 and 14):

$$P_{trans} = \beta \times r_{PRB} + \sigma, \tag{4}$$

where β and σ denote the slope and offset, respectively. As shown in Supplementary Tables 21 and 22, base stations of different types also have different coefficients. By substituting equation (4) into equation (3), we obtain the relationship between RRU power (P_{RRU}) and r_{PRB}. Given a base station's traffic load L, r_{PRB} can be approximated as L/C, where C denotes the base station's capacity. Alternatively, when a base station is in sleep mode, its RRU power becomes independent of its traffic load and principally distributed into a small interval (Supplementary Fig. 15). We use the average value to approximate the RRU power in sleep mode for different base station types (Supplementary Table 23). Moreover, the power consumption of the cooling devices is simulated using EnergyPlus[30], a widely used program developed by Lawrence Berkeley National Laboratory (see Supplementary Note 2 for the details).

Carbon emission estimation model

Electricity dispatch model. Electricity dispatching, which selects available generating units in a region to meet the power loads, is typically used to schedule the amount of power each plant generates. In this paper, we formulated a day-ahead unit commitment model to quantify the thermal coal consumption of power plants, which is expressed as a linear programming optimization problem:

$$\min_{X} \sum_{i\in\Phi}\sum_{t\in T}[c_i^{power}x_i^{power}(t) + c_i^{up}x_i^{up}(t) + c_i^{down}x_i^{down}(t)], \tag{5}$$

subject to:

$$\sum_{i\in\Phi} x_i^{power}(t) + P_{outside}(t) = P_{load}(t)/(1-r_{loss}), \forall t \in T, \tag{6}$$

$$P_i^{min}x_i^{on/off}(t) \le x_i^{power}(t) \le P_i^{max}x_i^{on/off}(t), \forall i \in \Phi, \forall t \in T, \tag{7}$$

$$\sum_{i\in\Phi} P_i^{max}x_i^{on/off}(t) \ge P_{res}(t), \forall t \in T, \tag{8}$$

$$\sum_{\tau=t}^{t+T_i^{up}-1} x_i^{on/off}(\tau) \ge T_i^{up}x_i^{up}(t), \forall i \in \Phi, \forall t \in T, \tag{9}$$

$$\sum_{\tau=t}^{t+T_i^{down}-1} [1 - x_i^{on/off}(\tau)] \ge T_i^{down}x_i^{down}(t), \forall i \in \Phi, \forall t \in T, \tag{10}$$

$$x_i^{up}(t) + x_i^{down}(t) \le 1, \forall i \in \Phi, \forall t \in T, \tag{11}$$

$$x_i^{up}(t) - x_i^{down}(t) = x_i^{on/off}(t) - x_i^{on/off}(t-1), \forall i \in \Phi, \forall t \in T, \tag{12}$$

$$x_i^{power}(t) \ge 0, \forall i \in \Phi, \forall t \in T, \tag{13}$$

$$x_i^{up}(t), x_i^{down}(t), x_i^{on/off}(t) \in \{0,1\}, \forall i \in \Phi, \forall t \in T, \tag{14}$$

where Φ is the set of coal-fired power units and $T = \{1, 2, \ldots, 48\}$ represents the time slots among a day's 48 half-hours. $X = \{x_i^{power}(t), x_i^{up}(t), x_i^{down}(t), x_i^{on/off}(t)\}$ are decision variables. $x_i^{power}(t)$ indicates the scheduled power generation of coal-fired power unit i at time slot t. $x_i^{up}(t)$ and $x_i^{down}(t)$ denote the startup and shutdown operations of coal-fired power unit i at time slot t. $x_i^{on/off}(t)$ denotes the on/off states of coal-fired unit i at time slot t. The objective of equation (5) is to minimize the total economic cost, including the power generation cost $c_i^{power}x_i^{power}(t)$, the startup cost $c_i^{up}x_i^{up}(t)$ and the shutdown cost $c_i^{down}x_i^{down}(t)$. Equation (6) represents the equilibrium between power generation and consumption. $P_{outside}(t)$ denotes the input power from outside regions. $P_{load}(t)$ denotes the local power load at time slot t. r_{loss} denotes the average loss rate of power transmission. Equation (7) specifies the upper and lower bounds of power generation. Equation (8) stipulates that the total capacity of working units must exceed the spinning reserve requirement $P_{res}(t)$. Equations (9) and (10) indicate that each unit must maintain a working state for at least half an hour. T_i^{up} and T_i^{down} denote the minimum on and off half-hours of power unit $i \in \Phi$. Equations (11) and (12) show the connections between startup/

shutdown operations and each power unit's on/off state. In equation (14), $x_i^{\mathrm{up}}(t) = 1$ indicates a startup operation, $x_i^{\mathrm{down}}(t) = 1$ indicates a shutdown operation and $x_i^{\mathrm{on/off}}(t) = 1$ indicates that power unit i is on.

In Nanchang, the source of electricity has two parts. One is from the local power plants distributed in Nanchang ($x_i^{\mathrm{power}}, i \in \Phi$), and the other is from the input power from outside regions (P_{outside}). The local power plants in Nanchang are controllable in the electricity dispatch model and support the energy consumption of mobile networks. According to the government report[31], Nanchang has three local power plants: the Nanchang plant, the Xinchang plant and the Hongping plant.

The annual development report of China's power industry[32] shows that the thermal coal consumption rate for the generation of energy with different capacities is

$$c_i^{\mathrm{coal}} = \begin{cases} 0.3007\,t\,MWh^{-1}, & P_i^{\max} > 300\,MW \\ 0.3357\,t\,MWh^{-1}, & P_i^{\max} \le 300\,MW \end{cases}. \tag{15}$$

By optimizing equation (5), the optimal scheduling strategies for coal-fired power units can be obtained. Let $x_i^{\mathrm{power}*}(t)$ denote the optimal solution. The total thermal coal consumption within one day, denoted by Q^{coal}, can be calculated as follows:

$$Q^{\mathrm{coal}} = \sum_{i\in\Phi}\sum_{t\in T}\frac{1}{2}c_i^{\mathrm{coal}}x_i^{\mathrm{power}*}(t). \tag{16}$$

The coefficient 1/2 refers to half an hour because the time slot, in our case, is half an hour.

Carbon emission estimation for mobile networks in Nanchang. To examine the carbon emissions from mobile networks, the total power load $P_{\mathrm{load}}(t)$ is divided into two parts:

$$P_{\mathrm{load}}(t) = P_{\mathrm{orig}}(t) + P_{\mathrm{BS}}(t), \forall t \in T, \tag{17}$$

where $P_{\mathrm{orig}}(t)$ is the residential and industrial power load excluding base station power load and $P_{\mathrm{BS}}(t)$ is the power dispatched to base stations to meet their operational needs. The difference in carbon emissions with and without $P_{\mathrm{BS}}(t)$ is used to characterize the carbon emission caused by mobile networks. Specifically, we first solve equation (5) with $P_{\mathrm{load}}(t) = P_{\mathrm{orig}}(t) + P_{\mathrm{BS}}(t)$ and obtain the optimal solution of power generation $x_i^{\mathrm{power}*(1)}(t)$. We next get the optimal solution of power generation $x_i^{\mathrm{power}*(2)}(t)$ with $P_{\mathrm{load}}(t) = P_{\mathrm{orig}}(t)$. In terms of equation (16), the thermal coal consumption of mobile networks within one day, denoted by $Q_{\mathrm{mobile}}^{\mathrm{coal}}$, is computed as follows:

$$Q_{\mathrm{mobile}}^{\mathrm{coal}} = \sum_{i\in\Phi}\sum_{t\in T}\frac{1}{2}c_i^{\mathrm{coal}}\left[x_i^{\mathrm{power}*(1)}(t) - x_i^{\mathrm{power}*(2)}(t)\right]. \tag{18}$$

We considered China's thermal coal, which consists of anthracite, bituminous, lignite and other types. Liu et al.[33] pointed out that China's thermal coal has low heating values ($h^{\mathrm{coal}} = 20.95\ \mathrm{GJ\ t^{-1}}$) compared with the global average heating value (29.3 GJ $\mathrm{t^{-1}}$) provided by the United Nations. The net carbon content per unit energy is $\alpha^{\mathrm{coal}} = 26.59\ \mathrm{tC\ TJ^{-1}}$, and the oxidization rate of thermal coal is set as $O^{\mathrm{coal}} = 99\%$. Thus, the emission factor of China's thermal coal, denoted by e^{coal}, is calculated as follows:

$$e^{\mathrm{coal}} = O^{\mathrm{coal}} \times h^{\mathrm{coal}} \times \alpha^{\mathrm{coal}} \times 3.67 = 2.02\ \mathrm{tCO_2\ t^{-1}}. \tag{19}$$

The carbon emissions from mobile networks, denoted by $Q_{\mathrm{mobile}}^{\mathrm{CO_2}}$, is computed as follows:

$$Q_{\mathrm{mobile}}^{\mathrm{CO_2}} = e^{\mathrm{coal}}Q_{\mathrm{mobile}}^{\mathrm{coal}}. \tag{20}$$

In practice, the $P_{\mathrm{orig}}(t)$ of Nanchang is approximated through the typical yearly and daily power load curves of Jiangxi province (see Supplementary Note 3 for the details). We also assumed that solar panels are installed on base stations, which can supply a portion of the base stations' power load. The power dispatched to a single base station is therefore expressed as

$$P_{\mathrm{BS},j}(t) = \begin{cases} \hat{P}_{\mathrm{BS},j}(t) - \mathrm{PV}_{\mathrm{BS},j}(t), & \text{if } \hat{P}_{\mathrm{BS},j}(t) > \mathrm{PV}_{\mathrm{BS},j}(t) \\ 0, & \text{otherwise} \end{cases}, \tag{21}$$

where $\hat{P}_{\mathrm{BS},j}(t)$ denotes the power load of base station j at time slot $t \in T$, $\mathrm{PV}_{\mathrm{BS},j}(t)$ denotes the power generated by the solar panel installed on base station j, and $P_{\mathrm{BS},j}(t)$ denotes the power dispatched to base station j from power plants. The power dispatched to base stations $P_{\mathrm{BS}}(t)$ can therefore be expressed as

$$P_{\mathrm{BS}}(t) = \sum_j P_{\mathrm{BS},j}(t). \tag{22}$$

Carbon emission estimation across provinces. We apply the Monte Carlo method to estimate the capacity of mobile networks in each province. We repeatedly and randomly sample base stations from the Nanchang set according to the number of 4G base stations and 5G base stations in each province. The Monte Carlo simulations are performed 1,000 times for each province. By adding each sampled base station's capacity and maximum energy consumption, we can obtain the total network capacity C_p and maximum energy consumption $E_{\max,p}$ of mobile networks in province p.

We next estimate the network traffic of each province. We assumed that, for a given month, the average traffic per user across regions is comparable. We thus determine the average traffic per user in Nanchang:

$$\bar{L} = (L_{4\mathrm{G}} + L_{5\mathrm{G}})/N_{\mathrm{user}}, \tag{23}$$

where $\bar{L}$ denotes the average traffic per user, $L_{4\mathrm{G}}$ and $L_{5\mathrm{G}}$ refer to the traffic load of 4G and 5G networks in Nanchang, and N_{user} denotes the number of mobile users in Nanchang (Supplementary Table 2). We next estimate provincial network traffic on the basis of the number of mobile users in each province (Supplementary Table 4):

$$L_p = \bar{L} \times N_{p,\mathrm{user}}, \tag{24}$$

where L_p and $N_{p,\mathrm{user}}$ denote the traffic load and the number of mobile users in province p, respectively.

Given the misalignment factor M_p of province p, the energy efficiency of the mobile network in province p when the network traffic load is L_p can be expressed as

$$\eta_p^{\mathrm{energy}}(L_p) = \frac{C_p/E_{\max,p}}{(1 + M_p/\tilde{L}_p)}, \tag{25}$$

where $\tilde{L}_p = L_p/C_p$ denotes the normalized traffic load. We estimate the misalignment factor M_p of province p on the basis of its normalized network traffic load and the energy-saving method it uses (see Supplementary Note 5 for the details). The energy consumption of the mobile network in province p, denoted by E_p, can be estimated as

$$E_p = E_{\max,p}(M_p + \tilde{L}_p). \tag{26}$$

According to Nanchang's results, the average grid emission factor is $\gamma^{\mathrm{CO_2}} = 0.68\ \mathrm{tCO_2\ MWh^{-1}}$, which has no significant difference before and after launching the 5G network (Supplementary Fig. 5). The carbon emissions of mobile networks in province p, denoted by $Q_{\mathrm{mobile},p}^{\mathrm{CO_2}}$, is thus computed as follows:

$$Q^{CO_2}_{\text{mobile},p} = E_p \times \gamma^{CO_2}. \quad (27)$$

Energy-saving method in mobile networks

DeepEnergy divides all cells into multiple grids and then trains reinforcement learning agents to decide whether each cell should enter sleep mode at each time step (see Supplementary Note 4 for the details). The reinforcement learning agents need to control the status of cells on the basis of the current state of the mobile network to reduce the total amount of energy consumption. This includes the energy consumed by RRUs and the energy consumed by BBUs and cooling devices. We model cell control as a multi-agent cooperation problem: each cell c_n is managed by an agent (agent_n), and these agents cooperate to minimize energy consumption.

The observation of each agent_n includes the feature vectors of other cells in the same base station or the same grid. The feature vector of cell c_n consists of time t; the traffic loads of the grid g_m that the cell c_n belongs to in the last four time steps, $(L^m_{t-4}, L^m_{t-3}, L^m_{t-2}, L^m_{t-1})$; and the device parameters of the cells in $\mathcal{N}^g_m \cup \mathcal{N}^b_k$. $\mathcal{N}^g_m$ denotes the set of cells in the grid g_m, and $\mathcal{N}^b_k$ denotes the set of cells of the base station BS_k that the cell c_n belongs to.

To encourage agents to work together, we set the reward for agent c_n to $r_n = -\sum_{n' \in \mathcal{N}^g_m} P^{\text{RRU}}_{n'} - P^{\text{BBU}}_k - P^{\text{cooling}}_k$ (see Supplementary Note 4 for the details). The first term indicates the energy of RRUs in cells that belong to the same grid as cell c_n. The second term indicates the energy of BBUs and cooling devices in the base station that cell c_n belongs to. We considered training a policy network to output the action on the basis of the current state to solve this multi-agent collaboration problem. However, the large number of agents is a major challenge. The large-scale agents lead to massive state space. When an agent makes the decision, it should efficiently integrate the states of other associated agents. For this problem, we constructed two graphs based on the intra-grid and intra-BS relationships and then used the graph neural network to integrate the information of the associated nodes (that is, agents) in the graphs. Large-scale agents also lead to complex interactions between agents, making the expected rewards of different actions difficult to estimate. We thus introduced the idea of mean field multi-agent reinforcement learning[34] to integrate the effects of other agents' decisions on the target agent and designed two masks to decrease the difficulty of action value estimation. The first mask denotes whether the grid's traffic demand can be met if the agent sets the respective cell to sleep. The second mask denotes whether all other cells under the same base station can sleep if the cell is set to sleep mode.

These masks are derived from the actions of other agents and can be used only as training input. Each agent therefore has two action-value networks, $q^2(\mathbf{o}_n, a, \mathbf{m}_n; \boldsymbol{\theta}^2_q)$ for training and $q^1(\mathbf{o}_n, a; \boldsymbol{\theta}^1_q)$ for inference, where $\mathbf{o}$ denotes the observation, a denotes the action, $\mathbf{m}$ denotes masks and $\boldsymbol{\theta}$ denotes the parameters of the action-value networks. In the execution stage, the action-value network without masks as input, $q^1(\mathbf{o}_n, a; \boldsymbol{\theta}^1_q)$, predicts the rewards associated with different actions, setting the cell to sleep or not, on the basis of the observation. Using the ϵ-greedy method, the agent determines the status of the cell by sampling the action on the basis of the predicted rewards. After the statuses of all cells determined by the agents are executed, the rewards for all agents are calculated. All agents' observations, actions and rewards are appended to the replay buffer. In the training stage, the action-value network with masks as input, $q^2(\mathbf{o}_n, a, \mathbf{m}_n; \boldsymbol{\theta}^2_q)$, is trained with the replay buffer to predict the rewards of different actions on the basis of the observation and masks. The network q^2 is optimized through the following loss function:

$$L_2 = \frac{1}{2}\left[q^2(\mathbf{o}_n, a, \mathbf{m}_n; \boldsymbol{\theta}^2_q) - r_n\right]^2, \quad (28)$$

where the mask $\mathbf{m}_n$ is obtained on the basis of the actions recorded in the replay buffer. The action-value network, $q^1(\mathbf{o}_n, a; \boldsymbol{\theta}^1_q)$, is then optimized by imitating the second network, $q^2(\mathbf{o}_n, a, \mathbf{m}_n; \boldsymbol{\theta}^2_q)$:

$$L_1 = \frac{1}{2}\sum_a \left[q^1(\mathbf{o}_n, a; \boldsymbol{\theta}^1_q) - q^2(\mathbf{o}_n, a, \mathbf{m}_n; \boldsymbol{\theta}^2_q)\right]^2, \quad (29)$$

where the mask $\mathbf{m}_n$ is calculated on the basis of the resampled actions. The resampling process is equivalent to the sampling process for the distribution of the mask vector. Thus, the first network q^1 would learn to predict the rewards of various actions under the sampled distribution of the mask vector. The framework of DeepEnergy is shown in Supplementary Fig. 19. The algorithm is shown in Supplementary Algorithm 1. Notably, after determining the working state of cells, we still need to redistribute the intra-grid network traffic among cells. The cells in each grid are equivalent in terms of service capability, and thus intra-grid network traffic can be flexibly transferred between cells within the grid. Specifically, given the working state of cells, we will then redistribute the intra-grid traffic of each active cell proportionally according to its capacity; namely, the cell with a higher capacity will carry more traffic.

Solar PV modelling and simulation

We used PVWatts[22,23], a PV system simulator developed by the National Renewable Energy Laboratory, to simulate the potential electricity generation of a PV system. We located PV panels using the coordinates of base stations and used the typical yearly meteorological data for the simulation. All other parameters were set to the default values, as PVWatts provides the most up-to-date standards for PV installations (see Supplementary Table 5 for the details).

The cost structure of a PV system is divided into the initial investment cost, the operation cost and the maintenance cost[35]. The initial investment cost includes PV modules, supporting structures, inverters, wiring, junction boxes, engineering costs (design, transportation and installation) and insurance. The annual operating costs are equivalent to 1% of system investment. The maintenance cost includes inverter replacement in the tenth year[36]. We assumed that the lifetime of the PV system is 20 years. The specific costs are listed in Supplementary Table 17; these are compiled from the China Photovoltaic Industry Association (China PV industry development roadmap; http://www.chinapv.org.cn/road_map.html). The cost data are real-world data collected from the PV industry of China by the China Photovoltaic Industry Association and under the guidance of the Ministry of Industry and Information Technology.

Reporting summary

Further information on research design is available in the Nature Portfolio Reporting Summary linked to this article.

Data availability

The numbers of base stations and mobile users in each province are listed in Supplementary Tables 3 and 4. The network traffic data and the number of mobile users in Nanchang are listed in Supplementary Table 2. Source data are provided with this paper.

Code availability

The code used in this study can be downloaded from https://github.com/Tong89/Sustainability_5G.

References

1. Manyika, J. & Roxburgh, C. *The Great Transformer: The Impact of the Internet on Economic Growth and Prosperity* (McKinsey Global Institute, 2011).
2. Dang, S., Amin, O., Shihada, B. & Alouini, M.-S. What should 6G be? *Nat. Electron.* **3**, 20–29 (2020).
3. Mwangama, J., Malila, B., Douglas, T. & Rangaka, M. What can 5G do for healthcare in Africa? *Nat. Electron.* **3**, 7–9 (2020).
4. Gohar, A. & Nencioni, G. The role of 5G technologies in a smart city: the case for intelligent transportation system. *Sustainability* **13**, 5188 (2021).

5. Dai, C., Liu, X., Lai, J., Li, P. & Chao, H.-C. Human behavior deep recognition architecture for smart city applications in the 5G environment. *IEEE Netw.* **33**, 206–211 (2019).
6. Taleb, T., Afolabi, I. & Bagaa, M. Orchestrating 5G network slices to support industrial internet and to shape next-generation smart factories. *IEEE Netw.* **33**, 146–154 (2019).
7. Al-Bawri, S. S., Islam, M. T., Islam, M. S., Singh, M. J. & Alsaif, H. Massive metamaterial system-loaded MIMO antenna array for 5G base stations. *Sci. Rep.* **12**, 14311 (2022).
8. Hecht, J. et al. The bandwidth bottleneck. *Nature* **536**, 139–142 (2016).
9. I, C.-L., Han, S. & Bian, S. Energy-efficient 5G for a greener future. *Nat. Electron.* **3**, 182–184 (2020).
10. Ding, Y. et al. Carbon emissions and mitigation potentials of 5G base station in China. *Resour. Conserv. Recycl.* **182**, 106339 (2022).
11. Tomás, J. P. *China Ends August with 2.1 Million 5G Base Stations: Report* (RCR Wireless News, 2022); https://www.rcrwireless.com/20220923/5G/china-ends-august-2-million-5G-base-stations-report
12. Griggs, D. et al. Sustainable development goals for people and planet. *Nature* **495**, 305–307 (2013).
13. Guo, J., Wang, L., Zhou, W. & Wei, C. Powering green digitalization: evidence from 5G network infrastructure in China. *Resour. Conserv. Recycl.* **182**, 106286 (2022).
14. Ilieva, R. T. & McPhearson, T. Social-media data for urban sustainability. *Nat. Sustain.* **1**, 553–565 (2018).
15. Yang, C., Li, J., Ni, Q., Anpalagan, A. & Guizani, M. Interference-aware energy efficiency maximization in 5G ultra-dense networks. *IEEE Trans. Commun.* **65**, 728–739 (2016).
16. Birdsey, R. A. *Carbon Storage and Accumulation in United States Forest Ecosystems* Vol. 59 (US Department of Agriculture, Forest Service, 1992).
17. Peng, C., Lee, S.-B., Lu, S., Luo, H. & Li, H. Traffic-driven power saving in operational 3G cellular networks. In *Proc. 17th Annual International Conference on Mobile Computing and Networking* (eds Ramanathan, P., Nandagopal, T. & Levine, B.) 121–132 (Association for Computing Machinery, 2011).
18. Rostami, S., Heiska, K., Puchko, O., Leppanen, K. & Valkama, M. Pre-grant signaling for energy-efficient 5G and beyond mobile devices: method and analysis. *IEEE Trans. Green Commun. Netw.* **3**, 418–432 (2019).
19. Wu, J., Zhang, Y., Zukerman, M. & Yung, E. K.-N. Energy-efficient base-stations sleep-mode techniques in green cellular networks: a survey. *IEEE Commun. Surv. Tutor.* **17**, 803–826 (2015).
20. Yu, G., Chen, Q. & Yin, R. Dual-threshold sleep mode control scheme for small cells. *IET Commun.* **8**, 2008–2016 (2014).
21. Chamola, V. & Sikdar, B. Solar powered cellular base stations: current scenario, issues and proposed solutions. *IEEE Commun. Mag.* **54**, 108–114 (2016).
22. Freeman, J. M. et al. *System Advisor Model (SAM) General Description* (National Renewable Energy Lab, 2018).
23. Waldman, J., Sharma, S., Afshari, S. & Fekete, B. Solar-power replacement as a solution for hydropower foregone in US dam removals. *Nat. Sustain.* **2**, 872–878 (2019).
24. Peng, W. et al. Managing China's coal power plants to address multiple environmental objectives. *Nat. Sustain.* **1**, 693–701 (2018).
25. Wang, J. et al. Exploring the trade-offs between electric heating policy and carbon mitigation in China. *Nat. Commun.* **11**, 6054 (2020).
26. Bogdanov, D. et al. Radical transformation pathway towards sustainable electricity via evolutionary steps. *Nat. Commun.* **10**, 1077 (2019).
27. *Statistics in Communication Industry* (People's Republic of China's Ministry of Industry and Information Technology, 2022); https://www.miit.gov.cn/gxsj/tjfx/txy/index.html
28. Arnold, O., Richter, F., Fettweis, G. & Blume, O. Power consumption modeling of different base station types in heterogeneous cellular networks. In *2010 Future Network & Mobile Summit* (ed. Saracco, R.) 1–8 (IEEE, 2010).
29. I, C.-L. et al. Toward green and soft: a 5G perspective. *IEEE Commun. Mag.* **52**, 66–73 (2014).
30. Crawley, D. B. et al. Energyplus: creating a new-generation building energy simulation program. *Energy Build.* **33**, 319–331 (2001).
31. *Notice of the Office of the People's Government of Nanchang City on Forwarding the 2021 Plan of the Municipal Development and Reform Commission and State Grid Nanchang Power Supply Company for Orderly Power Consumption of Nanchang Power Grid* (Nanchang Municipal People's Government, 2021); http://www.nc.gov.cn/nc_xxgk/jsp/zfgb/ncgb_content.jsp?mid=a731211fe1094abfaea8ab348bd5ba8b
32. China Electricity Council *Annual Development Report of China's Power Industry (2021)* 1st edn (China Building Materials Press, 2021).
33. Liu, Z. et al. Reduced carbon emission estimates from fossil fuel combustion and cement production in China. *Nature* **524**, 335–338 (2015).
34. Yang, Y. et al. Mean field multi-agent reinforcement learning. In *International Conference on Machine Learning* (eds Dy, J. G. & Krause, A.) 5571–5580 (PMLR, 2018).
35. Yan, J., Yang, Y., Elia Campana, P. & He, J. City-level analysis of subsidy-free solar photovoltaic electricity price, profits and grid parity in China. *Nat. Energy* **4**, 709–717 (2019).
36. Kaabeche, A., Belhamel, M. & Ibtiouen, R. Techno-economic valuation and optimization of integrated photovoltaic/wind energy conversion system. *Sol. Energy* **85**, 2407–2420 (2011).

Acknowledgements

This research has been supported in part by the National Key Research and Development Program of China under grant no. 2020YFA0711403 to D.J., by the National Natural Science Foundation of China under grant no. U21B2036 to T.J., by the National Natural Science Foundation of China under grant no. 61971267 to Y.L., and the International Postdoctoral Exchange Fellowship Program (Talent Introduction Program) under Project YJ20210274 to T.L. The individuals or organizations who provided funding had no role in study design, data collection, analysis, publication decision or preparation of the paper. We also thank the China Mobile Research Institute for Jiutian platform support and the China Mobile Group Jiangxi Company for data support.

Author contributions

T.L., D.J., Y.L. and T.J. conceived and designed the study. L.Y. and Y.Z. collected and provided the data. T.L., Y.M., T.D. and W.H. carried out the simulations and analyses. All authors contributed to the discussions on the methods and the writing of this article.

Competing interests

The authors declare no competing interests.

Additional information

Supplementary information The online version contains supplementary material available at https://doi.org/10.1038/s41893-023-01206-5.

Correspondence and requests for materials should be addressed to Yong Li or Tao Jiang.

Peer review information *Nature Sustainability* thanks Dusit Niyato and Jing Meng for their contribution to the peer review of this work.

nature portfolio

Corresponding author(s): Prof. Yong Li
Prof. Tao Jiang

Last updated by author(s): Jul 6, 2023

Reporting Summary

Nature Portfolio wishes to improve the reproducibility of the work that we publish. This form provides structure for consistency and transparency in reporting. For further information on Nature Portfolio policies, see our Editorial Policies and the Editorial Policy Checklist.

Statistics

For all statistical analyses, confirm that the following items are present in the figure legend, table legend, main text, or Methods section.

n/a	Confirmed
☐	☒ The exact sample size (*n*) for each experimental group/condition, given as a discrete number and unit of measurement
☐	☒ A statement on whether measurements were taken from distinct samples or whether the same sample was measured repeatedly
☒	☐ The statistical test(s) used AND whether they are one- or two-sided *Only common tests should be described solely by name; describe more complex techniques in the Methods section.*
☒	☐ A description of all covariates tested
☒	☐ A description of any assumptions or corrections, such as tests of normality and adjustment for multiple comparisons
☐	☒ A full description of the statistical parameters including central tendency (e.g. means) or other basic estimates (e.g. regression coefficient) AND variation (e.g. standard deviation) or associated estimates of uncertainty (e.g. confidence intervals)
☒	☐ For null hypothesis testing, the test statistic (e.g. *F*, *t*, *r*) with confidence intervals, effect sizes, degrees of freedom and *P* value noted *Give P values as exact values whenever suitable.*
☒	☐ For Bayesian analysis, information on the choice of priors and Markov chain Monte Carlo settings
☒	☐ For hierarchical and complex designs, identification of the appropriate level for tests and full reporting of outcomes
☒	☐ Estimates of effect sizes (e.g. Cohen's *d*, Pearson's *r*), indicating how they were calculated

Our web collection on statistics for biologists contains articles on many of the points above.

Software and code

Policy information about availability of computer code

Data collection	EnergyPlus 22.2.0 is used to collect weather data. For all the other data, we download them in the website without any software.
Data analysis	EnergyPlus 22.2.0 is used to analyze energy consumption of the cooling system. Python 3.6, PuLP 2.6, numpy1.19.5, pandas1.0.4 are used to analyze electricity dispatch. Python 3.7, Pytorch 1.11.0 and CUDA 10.2 is used to build DeepEnergy model. PVWatts 8.0 is used to simulate the potential electric generation of a PV system. Pyecharts 1.9.0 is used to depict the base map of China.

For manuscripts utilizing custom algorithms or software that are central to the research but not yet described in published literature, software must be made available to editors and reviewers. We strongly encourage code deposition in a community repository (e.g. GitHub). See the Nature Portfolio guidelines for submitting code & software for further information.

Data

Policy information about availability of data

All manuscripts must include a data availability statement. This statement should provide the following information, where applicable:

- Accession codes, unique identifiers, or web links for publicly available datasets
- A description of any restrictions on data availability
- For clinical datasets or third party data, please ensure that the statement adheres to our policy

The number of base stations and mobile users in each province are listed in Supplementary Tables 3 and 4. The network traffic data and the number of mobile users

in Nanchang are listed in Supplementary Table 2. All data are available from the corresponding author upon reasonable request. The code used in this study can be downloaded from https://github.com/Tong89/Sustainability_5G.

Research involving human participants, their data, or biological material

Policy information about studies with human participants or human data. See also policy information about sex, gender (identity/presentation), and sexual orientation and race, ethnicity and racism.

Reporting on sex and gender	Our study is not relevant with human characteristics such as sex and gender.
Reporting on race, ethnicity, or other socially relevant groupings	Our study has no socially relevant such as race and ethnicity.
Population characteristics	Our study is not relevant with population characteristics.
Recruitment	We do not have human participants in this work.
Ethics oversight	Our study is not relevant with this issue.

Note that full information on the approval of the study protocol must also be provided in the manuscript.

Field-specific reporting

Please select the one below that is the best fit for your research. If you are not sure, read the appropriate sections before making your selection.

☐ Life sciences ☐ Behavioural & social sciences ☒ Ecological, evolutionary & environmental sciences

For a reference copy of the document with all sections, see nature.com/documents/nr-reporting-summary-flat.pdf

Ecological, evolutionary & environmental sciences study design

All studies must disclose on these points even when the disclosure is negative.

Study description	To quantify carbon emissions induced by mobile networks, we propose a simulation-based model considering both the mobile communication system and the power generation system. We show that the launch of 5G networks exacerbates the misalignment between cellular traffic and energy consumption, which reduces carbon efficiency. To mitigate the misalignment and improve energy efficiency, we propose DeepEnergy, an energy-saving method leveraging collaborative deep reinforcement learning. We further assess the effects of adopting renewable energy and discover that the mobile network could accomplish more than 50% of its net-zero goal by integrating DeepEnergy and solar energy systems. Our study provides insight into carbon emission mitigation in 5G network infrastructure launching in China and overworld, paving the way towards achieving sustainable development goals and future net-zero mobile networks.
Research sample	The data used in this paper are collected from open-access websites and publications, and the projects collaborated with China Mobile Research Institute. The public can access all the datasets.
Sampling strategy	We apply the Monte Carlo method to estimate the capacity of mobile networks in each province. We repeatedly and randomly sample base stations from the Nanchang set according to the number of 4G base stations and 5G base stations in each province. The Monte Carlo simulations are performed 1,000 times for each province.
Data collection	In this paper, the energy consumption data of base stations and network traffic data in Nanchang are collected by the China Mobile Research Institute. The number of base stations and mobile users in each province are collected from the Ministry of Industry and Information Technology of the People's Republic of China. The outdoor air temperature data are collected from the World Meteorological Organization's weather dataset. The specific costs of PV system are compiled from the China Photovoltaic Industry Association (China PV industry development roadmap; http://www.chinapv.org.cn/road_map.html).
Timing and spatial scale	The energy consumption data of base stations are collected from from 300 4G base stations and 266 5G base stations in real-world mobile networks over one week in May 2022. The network traffic data in Nanchang are collected from January 2021 to May 2022. The number of base stations and mobile users are collected from January 2021 to May 2022.
Data exclusions	No data are excluded.
Reproducibility	The code used in this study can be downloaded from https://github.com/Tong89/Sustainability_5G.
Randomization	This is not relevant because we do not need to allocate the data into experimental groups.
Blinding	No blinding was performed since outcome data were required for model development.

Did the study involve field work? ☐ Yes ☒ No

Reporting for specific materials, systems and methods

We require information from authors about some types of materials, experimental systems and methods used in many studies. Here, indicate whether each material, system or method listed is relevant to your study. If you are not sure if a list item applies to your research, read the appropriate section before selecting a response.

Materials & experimental systems

n/a	Involved in the study
☒	☐ Antibodies
☒	☐ Eukaryotic cell lines
☒	☐ Palaeontology and archaeology
☒	☐ Animals and other organisms
☒	☐ Clinical data
☒	☐ Dual use research of concern
☒	☐ Plants

Methods

n/a	Involved in the study
☒	☐ ChIP-seq
☒	☐ Flow cytometry
☒	☐ MRI-based neuroimaging